Korean J. Chem. Eng., **31**(12), 2183-2191 (2014)
DOI: 10.1007/s11814-014-0142-z

pISSN: 0256-1115
eISSN: 1975-7220

Role of copper pyrovanadate as heterogeneous photo-Fenton like catalyst for the degradation of neutral red and azure-B: An eco-friendly approach

Sangeeta Kalal*, Narendra Pal Singh Chauhan, Noopur Ameta*, Rakshit Ameta***, Sudhish Kumar****, and Pinki Bala Punjabi*,†**

*Photochemistry Laboratory, Department of Chemistry, M. L. Sukhadia University, Udaipur - 313001, Rajasthan, India
**Department of Chemistry, B. N. P. G. College, Udaipur - 313001, Rajasthan, India
***Department of Chemistry, Pacific College of Basic & Applied Sciences, PAHER University, Udaipur - 313024, Rajasthan, India
****Department of Physics, University College of Science, M. L. Sukhadia University, Udaipur - 313001, Rajasthan, India
(*Received 2 October 2013 • accepted 21 May 2014*)

Abstract−The heterogeneous photo-Fenton like process is a green chemical pathway. It has an edge over conventional Fenton and photo-Fenton processes as it does not require the removal of ferrous/ferric ions in the form of sludge. We prepeared copper pyrovanadate or Volborthite ($Cu_3V_2(OH)_2O_7 \cdot 2H_2O$) composite photocatalyst by wet chemical method. The photocatalyst was characterized by SEM, XRD, IR, TGA/DSC, EDX and BET. Experiments demonstrated that catalyst could effectively catalyze degradation of neutral red and azure-B in presence of H_2O_2 in visible light. Moreover, the photo-Fenton-like catalytic activity of $Cu_3V_2(OH)_2O_7 \cdot 2H_2O$ was much higher than CuO and V_2O_5, when used alone as photocatalyst. The effect of variation of different parameters, i.e., pH, amount of photocatalyst, concentration of dye, amount of H_2O_2 and light intensity was also investigated. The degradation was well fitted under pseudo-first-order reaction with a rate constant of 2.081×10^{-4} sec^{-1} and 3.876×10^{-4} sec^{-1} for neutral red and azure-B, respectively. Quality parameters of dye solutions before and after photo-Fenton degradation were also determined. A tentative mechanism involving $^{\bullet}OH$ radical as an oxidant has been proposed. The high catalytic activity may be due to the $Cu_3V_2(OH)_2O_7 \cdot 2H_2O$ shell, which not only increased the surface hydroxyl groups, but also enhanced the interfacial electron transfer. The catalyst has been found to possess good recyclability.

Keywords: Advanced Oxidation Processes, Heterogeneous, Photo-Fenton, Neutral Red, Azure-B, Mechanism

INTRODUCTION

Production of wastewater in industrial processes is sometimes unavoidable, and in most cases a process to reduce the organic load and other contaminants must be employed before water discharge. The textile industry uses approximately 21-377 m^3 of water per ton of textile produced, and thus generates large quantities of wastewater from different steps of dyeing and finishing processes [1]. The major environmental concern is the removal of color from textile and dyestuff manufacturing wastewater. Pagga and Brown [2] reported that out of 87 dye stuffs only 47% are biodegradable.

It is difficult to treat and decolorize textile dye waste containing reactive dyes by conventional chemical and biological methods. To develop an efficient method for converting such dyestuffs into harmless products, advanced oxidation processes (AOPs) have been widely applied in recent years. AOPs have provided innovative, cost-effective catalyzed chemical oxidation for treating pollutants in low or high concentration from contaminated soil, sludge and water. AOPs are based on the generation of hydroxyl radical ($HO^{\bullet}$) in the homogeneous or heterogeneous phase, which has a high oxidation potential (2.8 V) that completely converts organic contaminant into CO_2, H_2O, inorganic ions or biodegradable compounds [3,4].

One well-known advanced oxidation process is the oxidation with Fenton and photo-Fenton reagent, where hydrogen peroxide reacts with ferrous ion and with ferric ion in presence of light, respectively, yielding powerful radicals, specially $HO^{\bullet}$ radicals which are able to oxidize the organic compounds in the following simplified manner (Eqs. (1)-(3)):

$$Fe^{2+} + H_2O_2 \rightarrow Fe^{3+} + HO^{\bullet} + OH^{-} \quad (1)$$

$$Fe^{3+} + H_2O \xrightarrow{h\nu} Fe^{2+} + HO^{\bullet} + H^{+} \quad (2)$$

$$HO^{\bullet} + \text{Organic matter} \rightarrow \text{Oxidation products} \quad (3)$$

The Fenton process has been used for the treatment of landfill leachate [5] and degradation of number of organic pollutants [6,7]. It has been reported that the combination of H_2O_2 and UV/Vis radiation with Fe(II) (photo-Fenton's process) can significantly improve the degradation of many organic compounds [8]. Photo-Fenton reactions are cyclic and on addition of H_2O_2, the process continues to generate more and more $HO^{\bullet}$ radicals, while in the Fenton process, reaction stops when all Fe^{2+} ions are consumed. In photo-Fenton reactions, two $HO^{\bullet}$ radicals are generated per ferric ion utilized and, hence, the rate of reaction is more than Fenton reaction. In this case, Fe^{3+} ions are not accumulated in the system.

The photodegradation of 2-chlorophenol (2-CP) using Fenton and the photo-Fenton processes has been reported by Hong et al. [9]. It has been observed that under the optimal conditions, the degradation efficiency of 2-CP in the photo-Fenton process was enhanced

†To whom correspondence should be addressed.
E-mail: pb_punjabi@yahoo.com

4% more than that of the Fenton process. The decomposition of azure-B by photo-Fenton reagent in the presence of ultrasound in homogeneous aqueous solution has been described by Vaishnave et al. [10]. The optimum rate constants for these reactions were determined as $k_1=2.99\times10^{-3}$ s^{-1} for photo-Fenton reaction and $k_2=4.39\times10^{-3}$ s^{-1} for sono-photo-Fenton reaction.

However, iron ions which act as catalyst get dissolved in water in the homogeneous Fenton process [11]. Due to this, the iron ions in the treated water normally exceed 10 mg/L and need to be removed, which adds to the cost as well as secondary pollution, thus limiting its industrial application [12].

To overcome drawbacks associated with homogeneous photo-Fenton process, heterogeneous photo-Fenton catalysts have been widely employed for the oxidation of organic pollutants. The major advantage of the use of heterogeneous catalytic materials is their easy recovery by simple filtration and reusability for further experiments.

Parida and Pradhan [13] reported Fe/meso-Al_2O_3 as an efficient photo-Fenton catalyst for the adsorptive degradation of phenol. The sample with 0.25 wt% Fe(II)/meso-Al_2O_3 was found to be an efficient catalyst, showing 98% degradation of 2.1×10^{-5} mol of phenol at pH 6 in 1 h. Kiwi et al. [14] prepared immobilized Fe-histidine complex on Nafion membrane and faded the color of azo dyes by photo-Fenton technology. The percentages of the homogeneous and heterogeneous processes leading to orange II disappearance on the Fe/histidine/Nafion surface have been quantified as a function of the pH. The results obtained indicate that at pH values>5.5, heterogeneous catalysis accounts for more than 96% of the orange II disappearance. Degradation of sunset yellow FCF using copper loaded bentonite and H_2O_2 as photo-Fenton like reagent has been reported [15]. At optimal conditions, the rate of degradation of sunset yellow FCF was obtained as $k=1.55\times10^{-4}$ sec^{-1}. Kumar et al. [16] reported a comparative study of degradation of dye intermediate (H-acid) using TiO_2/UV/H_2O_2 and photo-Fenton process. They observed that heterogeneous photocatalysis is a prominent method for degradation of dyes and dye intermediates containing industrial wastewaters. Sharma et al. [17] reported the degradation of Bismarck brown-R using copper loaded neutral alumina as heterogeneous photo-Fenton like reagent. Ameta et al. [18] studied the degradation of Coomasie brilliant blue R-250 by using copper-modified iron oxide as heterogeneous photo-Fenton reagent. The photodegradation efficiency after 2 hours of illumination was be 63%. Iurascu et al. [19] reported that almost complete degradation of phenol in water through a heterogeneous photo-Fenton process catalyzed by Fe-treated laponite was possible within 5 min. The catalyst prepared by thermal treatment and calcined at 350 °C showed the best catalytic performance.

Mixed oxides based on vanadium have been studied for their many technological applications, like lithium rechargeable battery and heterogeneous catalyses [20]. It has been reported that the introduction or combination of non-iron metals into the metal oxide structure to form multi-metal compounds could promote the Fenton like catalytic activity of the metal oxides in the oxidation of organic pollutants [21-25]. Vanadium (V), present in many compounds, for example V_2O_5 [26], V-MCM [27], $V_xSi_{4x}O_{6\cdot4x}$ [28], VO core containing complexes [29], and 1,2- $H_2SiV_2W_{10}O_{40}$ [30], can heterogeneously or homogeneously catalyze the oxidation of various organic and inorganic compounds by H_2O_2 in Fenton-like pathways [31].

Copper pyrovanadate compounds are of particular interest as cathode materials in lithium batteries and electrochromic devices [32]. Copper pyrovanadate was found for the first time to achieve the high catalytic activity for the decomposition of sulfuric acid to evolve O_2 at moderate temperatures around 650 °C, which is essential for the development of solar thermochemical water splitting cycles [33]. However, copper pyrovanadate has not been reported as a photo-Fenton like catalyst till now. Its high catalytic activity may be due to the $Cu_3V_2(OH)_2O_7\cdot2H_2O$ shell, which not only increased the surface hydroxyl groups, but also enhanced the interfacial electron transfer. It may also be due to the synergistic activation by both copper and vanadium ions.

Various photocatalysts have been used to degrade neutral red and azure-B. Their comparative activities have been reported in Table 1.

In this study, we prepared copper pyrovanadate by wet method. Instrumental analysis with FT-IR, XRD, SEM-EDX and BET techniques was used for structural study of the catalyst. The effect of heterogeneous photo-Fenton like catalyst for degradation of neutral red and azure-B dyes under visible light irradiation was studied in detail.

EXPERIMENTAL

1. Materials

Ammonium metavanadate (Himedia), copper nitrate trihydrate (Himedia), neutral red dye (LOBA Chemie Industrial Co.), azure-B dye (Himedia) and hydrogen peroxide (CDH, 30% w/v) were used as received commercially. All the chemicals used were of analytical grade.

Neutral red ($C_{15}H_{17}ClN_4$, MW 288.78, λ_{max}=520 nm), a phenazine

Table 1. A comparison of catalytic activity

Catalyst	Nature	Dye	k (Rate constant)	% Degradation efficiency	Ref.
La_2CoO_4	Photocatalyst	Azure-B	2.09×10^{-4} (s^{-1})	-	[34]
Bi_2O_3	Photocatalyst	Azure-B	16.16×10^{-5} s^{-1}	-	[35]
$BaCrO_4$	Photocatalyst	Azure-B	-	47% (after 2 h)	[36]
Zeolite-Arthrobacter viscosus system	Hybrid system	Azure-B	-	99% (after 8 day)	[37]
Potassium trisoxalatoferrate (III)	Homogeneous photo-Fenton system	Neutral red	5.04×10^{-5} sec^{-1}		[38]
ZnO/Fenton process		Neutral red	-	90% (after 8 h)	[39]
Cu–modified Fe_2O_3	Heterogeneous photo-Fenton	Neutral red	-	64% (after 2 h)	[40]

dye, has been used as an important coloring agent for its aqueous solution is deep red. Neutral red is often used as linsey-woolsey coloring agent, biological stain and acid-base indicator. Therefore, neutral red (NR) is an important constituent in dyeing wastewater. Azure-B ($C_{15}H_{16}ClN_3S$, MW 305.83, λ_{max}=550 nm) is an easily available phenothiazinium dye and has been widely employed both in metal determination and DNA staining detection [41]. Phenothiazinium dyes are photocytotoxic, and can cause photoinduced mutagenic effects [42].

2. Preparation of Catalyst

$Cu_3V_2(OH)_2O_7 \cdot 2H_2O$ was prepared by wet chemical process. Copper nitrate aqueous solution (0.1 M) was quickly poured into a (0.2 M) aqueous solution of NH_4VO_3 maintained at 75 °C under stirring. This mixture immediately led to a yellow precipitate. After 1 h reaction with continuous stirring, the color of the precipitate changed to green. It was then isolated by filtration, washed several times with pure water and methanol and dried at room temperature overnight.

3. Photo-Fenton Activity

For the photo-Fenton degradation, stock solution of dyes (1.0×10^{-3} M) were prepared. A reaction mixture containing dye (1.0×10^{-5} M), catalyst and hydrogen peroxide, was exposed to light for a certain period of time. A 200 W tungsten lamp (Philips) was used for irradiation purpose. The intensity of light at various distances was measured by "Suryamapi" [CEL Model 201]. *p*H of the solution was measured by a digital *p*H meter [Systronics Model 335]. *p*H of the solution was adjusted by using standard 0.1 N sulfuric acid and 0.1 N sodium hydroxide solutions. A Pyrex glass reactor of size (150 mm ×75 mm) with 1 L capacity whose surface area is 176 cm^2 was directly exposed to the light source. A water filter was used to cut off thermal radiations. Most of the experiments were conducted thrice in identical conditions, and the difference in the error between consecutive experiments was less than 2%. The entire photoreactor system was maintained at 25 °C with a thermostat (Fig. 1(a)). UV-VIS spectrophotometer [Systronics Model 106] was used for measuring absorbance of the reaction mixture at regular time intervals.

For the control experiments, equal amount of dye solution (1.0×10^{-5} M) was taken in five beakers (Fig. 1(b) and 1(c)).

1. In the first beaker only dye solution was taken and exposed to light.
2. In the second beaker H_2O_2 was added to the dye solution and exposed to light.
3. In the third beaker, 0.05 g copper pyrovanadate as catalyst was added to the dye solution and exposed to light.
4. In the fourth beaker both catalyst and H_2O_2 were added to the dye solution and kept in the dark.
5. In the fifth beaker both catalyst and H_2O_2 were added to the dye solution and exposed to the light.

The absorbance of reaction mixture in each beaker was measured with a spectrophotometer at regular time intervals. The absorbance of the reaction mixture for first four beakers had no significant change as compared to their initial absorbance. However, absorbance of reaction mixture in fifth beaker had considerable decrease in absorbance as compared to its initial value, indicating that copper pyrovanadate, H_2O_2 and light together accelerate the degradation of dyes.

It was observed that the absorbance of the solution decreases with increasing time intervals, which indicates that the concentration of neutral red and azure-B dyes decreases with increasing time of exposure. A plot of 2+log A versus time was linear and follows pseudo-first order kinetics (Typical runs Fig. 2). The rate constant was measured using the following expression:

$$k=2.303\times\text{Slope}$$

The chemical oxygen demand (COD) of reaction mixture before and after treatment was determined by redox method using ferrous ammonium sulfate and $KMnO_4$. The photodegradation efficiency

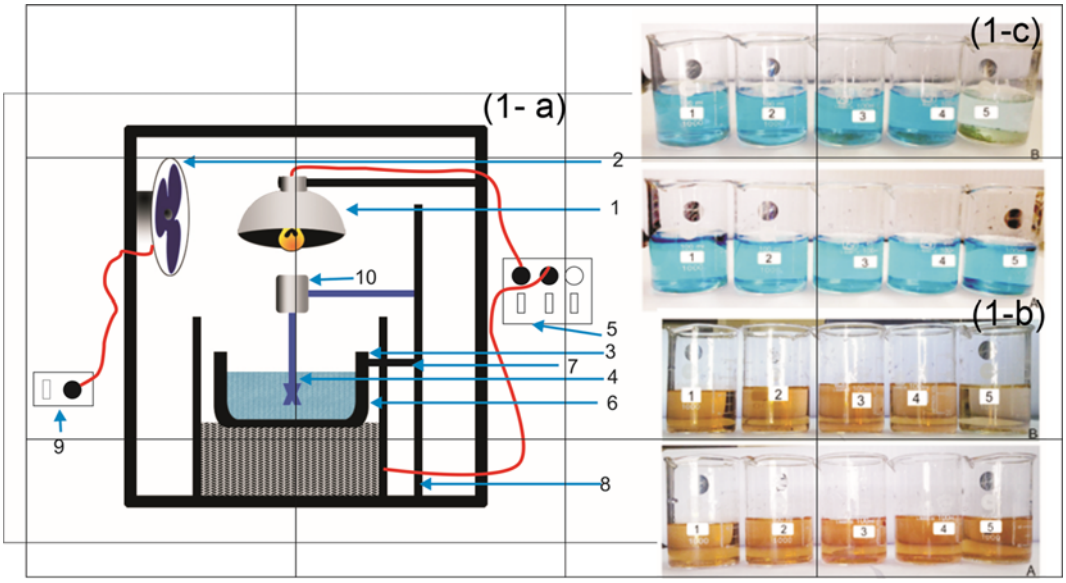

Fig. 1. (a) Schematic diagram of the experimental set-up: (1) tungsten lamp; (2) fan; (3) Pyrex glass reactor; (4) experimental solution; (5 and 9) switch box with stabilizers; (6) thermostat; (7) clamp; (8) stand; (10) motor.), (b) Discoloration of Neutral red in aqueous dispersions (A) before degradation (1) (2) (3) (4) (5) (B) after degradation (1) (2) (3) (4) (5), (c) Discoloration of Azure-B in aqueous dispersions (A) before degradation (1) (2) (3) (4) (5) (B) after degradation (1) (2) (3) (4) (5).

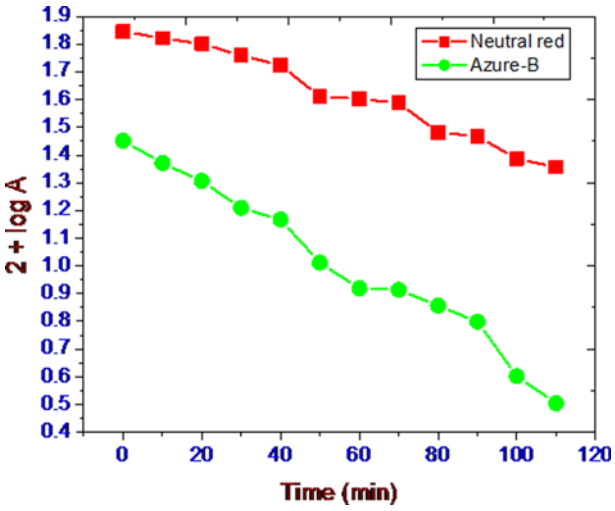

Fig. 2. Typical Runs (plotted between time and 2+log A at optimum conditions for [Neutral red]=7×10^{-5} M, pH=8.0, Catalyst=0.05 g, H_2O_2=0.40 mL, Light intensity=70.0 mWcm^{-2} and [Azure-B]=1.2×10^{-5} M, pH=6, Catalyst=0.06 g, H_2O_2= 0.50 mL, Light intensity=60.0 mWcm^{-2}).

of the catalyst was calculated from the following expression:

$$\eta = \frac{COD_{before} - COD_{after}}{COD_{before}} \times 100$$

η=photodegradation efficiency (%), COD_{before}=COD of dye solution before illumination and COD_{after}=COD of dye solution after illumination

Other quality parameters--dissolved oxygen, conductivity, salinity and total dissolved solids were measured using water analyzer (Systronics Model 371).

Powder of the catalyst after use was separated with centrifugation and washed with plenty of water. The washed slurry was dried at 80 °C in an oven for 5 h and used again for further degradation, which confirms its reusability.

Infrared (IR) spectra were recorded with a Perkin Elmer FTIR-1730 spectrometer with KBr disks at room temperature in the range of 4,000-400 cm^{-1}. FT-RAMAN spectrometer was a multi RAM BRUKER RFS 27, stand-alone model. The spectral range was 4,000-50 cm^{-1} with resolution of 2 cm^{-1}. The laser source was Nd : YAG 1,064 nm. The spectrometer has a large sample compartment to accommodate different sample formats, from powders to liquids in vials. The thermogravimetric analysis (TGA) was performed on a Perkin Elmer TGA- Pyris-1 thermogravimetric analyzer at a heating rate of 10 °C/min. The sample was kept in N_2 atmosphere to avoid oxidation during the entire heating process. Phase identification was carried out by X-ray diffraction (XRD) with a D/MAX-IIIA, Rigaku, Japan using Cu Kα radiation at 35 kV, 30 mA and 2θ=10-80°. Scanning electron microscopy (SEM) studies were performed using a Bruker AXS microscope equipped with energy dispersive X-ray (EDX) fluorescence spectral analysis for element composition and Robinson secondary electron (SE) and backscattered electron (BSE) detectors for imaging. The sample was placed on an adhesive carbon slice and coated with Au-Pd alloy 10 nm thick layer.

The surface area of the sample was determined by nitrogen adsorption/desorption analysis. The instrument utilized for nitrogen

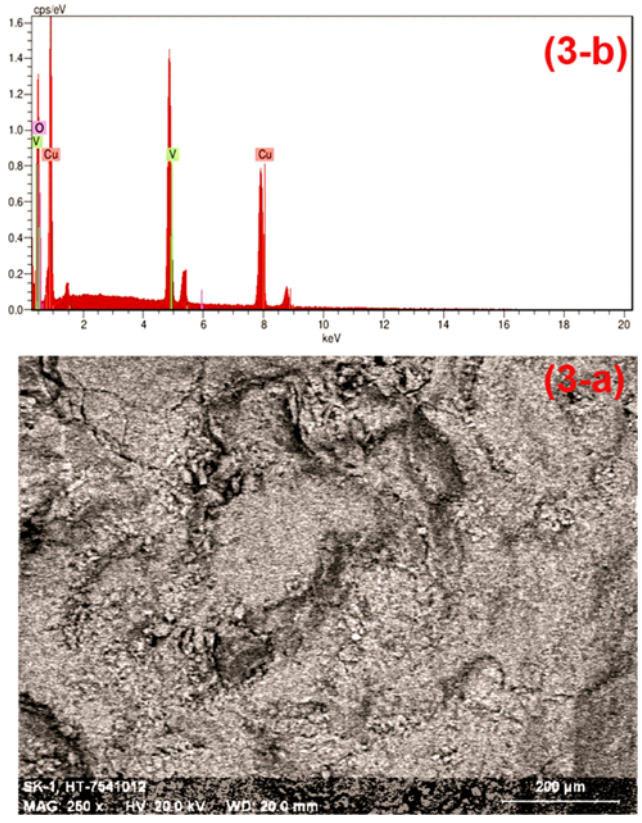

Fig. 3. (a) SEM image of catalyst, (b) EDX of catalyst.

sorption analysis was a Micromeritics (Gemini 2370), USA Surface Area Analyzer. Before each experiment, the sample (0.2 g) was degassed at 105 °C for 24 h. Stability of the catalyst was checked by atomic absorption spectroscopy using ETCL4129A atomic absorption spectrophotometer.

RESULTS AND DISCUSSION

1. Characterization Results

Scanning electron microscopy (SEM) of $Cu_3V_2(OH)_2O_7\cdot2H_2O$ is shown in (Fig. 3(a)). The basic structure of catalyst (volborthite) is a sheet-like structure with copper oxide/hydroxide layers that are held together by the pyrovanadate groups, and then these layers are stacked by layers of water. Based on the SEM image, porosity of the surface is evident and it seems that the particles have not grown with uniform size. The particle size of $Cu_3V_2(OH)_2O_7\cdot2H_2O$ that was propagated on the surface seems to be in the range of 50-200 µm. The surface looks rough and nearly fully covered with the particles grown on it. Further, it can also be seen from the SEM result that in addition to the larger particles, the surface contains some smaller particles as down to 20 µm or less. However, the appearance of bigger particles on the surface looks to be dominant. The aggregation of the smaller particles (in the nm range) may result in bigger $Cu_3V_2(OH)_2O_7\cdot2H_2O$ particles on the surface.

The specific surface area of the catalyst was measured by means of conventional BET method. Results showed that the average specific surface area of $Cu_3V_2(OH)_2O_7\cdot2H_2O$ particle was 17.6 m^2/g at 105 °C. This value may be attributed to the enhanced crystalline

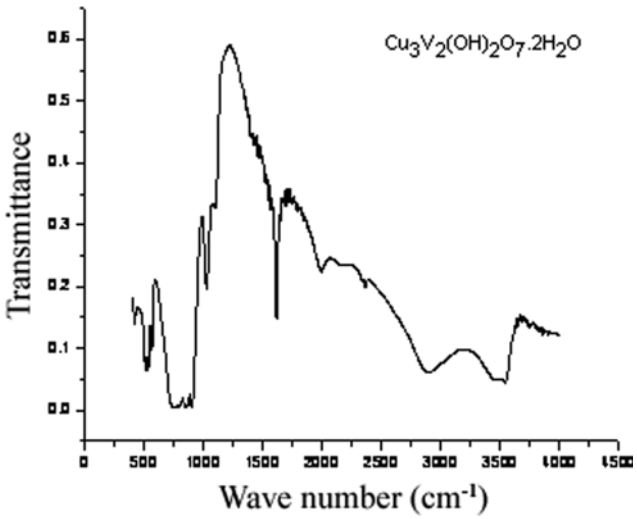

Fig. 4. FT-IR spectrum of catalyst.

grain size calcined at 750 °C.

The EDX analysis was performed for further confirmation of the obtained product composition (Fig. 3(b)) shows EDX spectrum, which indicates the existence of V (23.35%), Cu (48.94%) and O (25.74%) elements in the prepared photocatalyst.

Surface properties, especially surface hydroxyl groups, are very important for the degradation of organic pollutants in heterogeneous catalytic reactions. The photocatalyst was further characterized with FTIR to elucidate the surface OH group. Cu-O bonding was confirmed by a band at 592 cm^{-1} in FT-IR (Fig. 4) of the catalyst, while Raman spectrum (Fig. 5) indicatedd a band at 887 cm^{-1}, which confirms the bonding between vanadium and oxygen.

In FTIR the band at 1,508 cm^{-1} was assigned to the bending vibration of adsorbed water. The wide band at 3,500-3,600 cm^{-1} was attributed to the stretching of OH groups of chemisorbed water. This fact suggested that after loss of the water adsorbed on the surface, the catalyst did not suffer from any obvious decomposition and had favorable thermal stability in the temperature range investigated. It has been proven that the surface hydroxyl groups are the active sites for adsorption, oxidation decomposition and hydroxyl radicals generation [43-45]. $Cu_3V_2(OH)_2O_7 \cdot 2H_2O$ has more OH groups than FeO-H_2O_2 and CuO-H_2O_2, and this fact is in agreement with the FTIR results. Thus $Cu_3V_2(OH)_2O_7 \cdot 2H_2O$ may exhibit higher catalytic activities for pollutants removal. The surface OH group content for $Cu_3V_2(OH)_2O_7 \cdot 2H_2O$, FeO-$H_2O_2$ and CuO-H_2O_2 was calculated to be 3.8, 2.5 and 2.1%, respectively.

Stability of the catalyst was checked by atomic absorption spectroscopy using an ECTL 4129A atomic absorption spectrophotometer. Even after one month, leaching of copper or vanadium ions from the catalyst was found to be negligible. Thus, catalyst was found to possess good stability for its use as heterogeneous photo-Fenton like reagents under visible range.

To investigate the thermal stability of catalyst its TG/DTG was determined. Fig. 6 shows TG-DTG curve of the thermal decomposition process of photocatalyst at a heating rate of 5 °C/min in the air from room temperature to 800 °C. The total weight loss of the catalyst was approximately 77% and the decomposition process can be divided into two distinct steps. From the structural study of copper pyrovanadate [46], it was suggested that the copper pyrovanadate can be described by the formulation $Cu_3V_2(OH)_2O_7 \cdot 2H_2O$. This formulation was found to be in good agreement with TG curve, which presents two breaks at 270 and 330 °C, which correspond to two weight loss steps: removal of physically adsorbed water of hydration and the loss of surface hydroxyl group. Fig. 6 shows that there was only one DTG peak with 12.02% weight loss at 238.19 °C and then the weight was maintained nearly steady in the range 238.19 to 800 °C. A weight loss of about 18% is observed from 238 °C to about 800 °C in the TG curve. Hence, it is plausible to conclude that the optimum calcinations temperature is about 800 °C.

XRD diffraction patterns of the samples were recorded on 18 KW X-Ray diffractometer using Cu Kα radiation. Diffraction patterns were recorded over the 2θ range from 10° to 90° with a step size of 0.05°. The diffraction peaks at 2θ angles appeared in the order

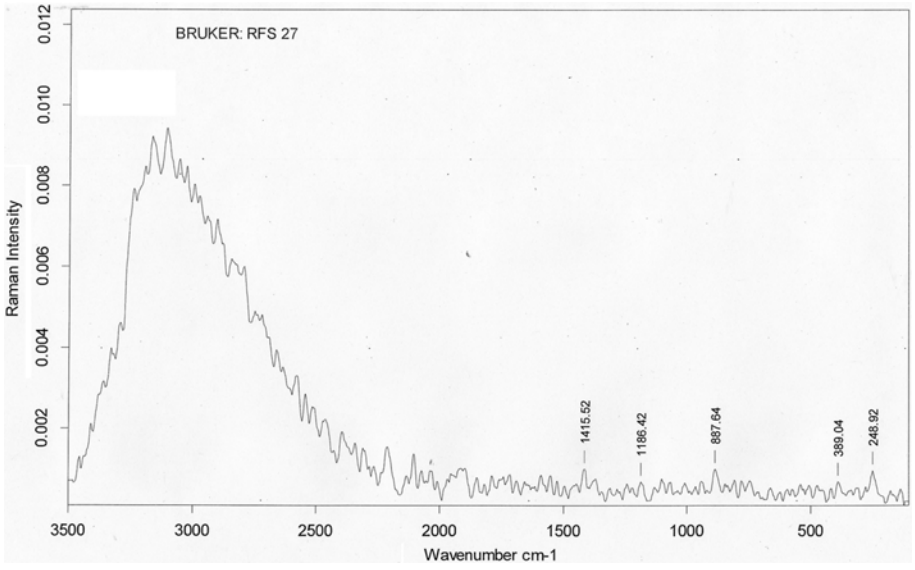

Fig. 5. Raman spectrum of catalyst.

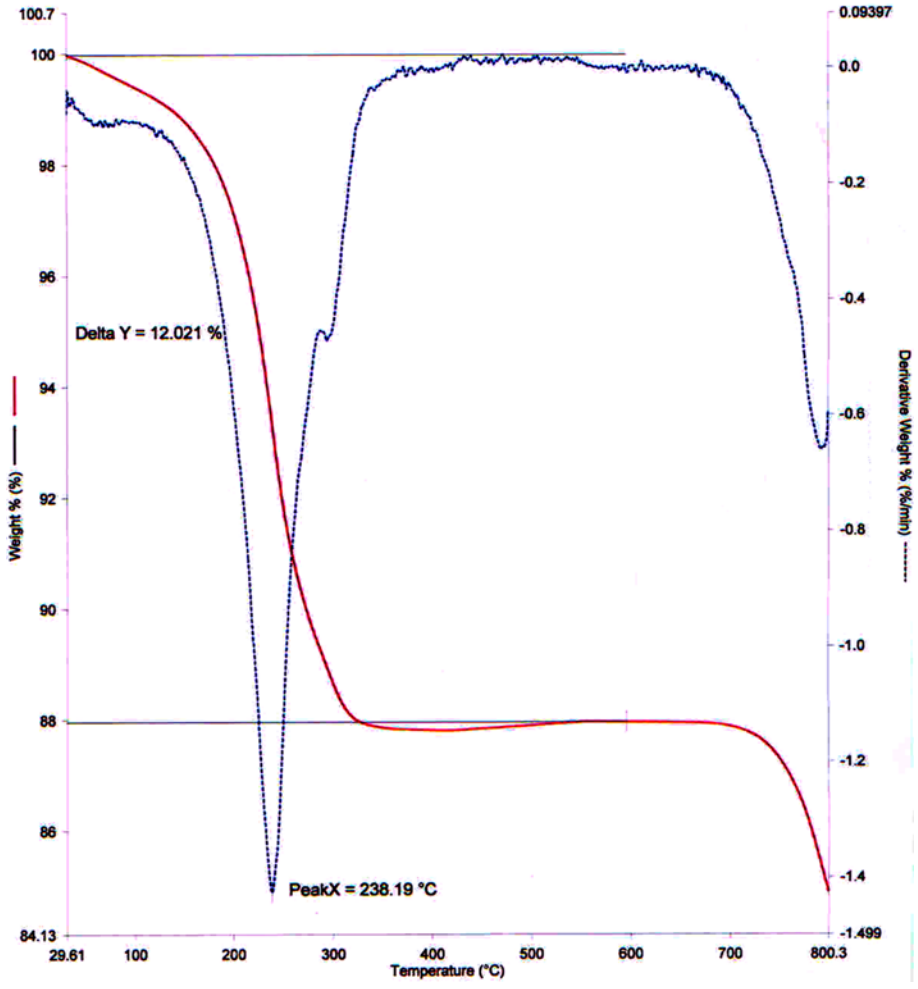

Fig. 6. TG-DTG curve of the thermal decomposition process of catalyst at a heating rate of 5 °C/min.

of 13.2°, 18.62°, 22.01°, 29.62°, 31.1°, 35.45°, 37.2°, 44.34°, 51.2° and 62.6° can be assigned to scattering from the (0 0 1), (1 1 0), (2 0 1), (2 0 2), (1 1 2), (2 2 0), (2 2 1), (1 0 2), (0 0 4) and (5 2 2) planes of the $Cu_3V_2(OH)_2O_7 \cdot 2H_2O$ type crystal lattice, respectively. From these diffraction peaks, the synthesized sample showed monoclinic crystalline structure compared with standard orthorhombic ammonium metavandate and rhombohedral copper nitrate trihydrate. The crystallite size (t) of the peak that appeared at 2θ=13° can be calculated by using Scherrer's formula, t=0.9 $\lambda/\beta \cos \theta$, where λ is the wavelength of X-rays used (1.5406 Å), β is the full width at half maximum (FWHM) and θ is the angle of diffraction. The average crystallite size of prepared nanopowder is found to be 82 nm, which is in the order of nanoscale.

2. Effect of Various Parameters

Effect of different parameters such as pH, concentration of dye, amount of H_2O_2, light intensity on photocatalytic activity has also been investigated.

It was anticipated that changes in pH would influence the degradation of the dye in two ways: (i) direct involvement of H^+ in the reaction at lower pH, and (ii) mass transport limitations imposed by the precipitation of a passive film on the metal surface at higher pH.

The effect of pH on photo-Fenton degradation of dyes was investigated in the pH range 5.0-8.5. With an increase in pH, the rate of reaction increased and after attaining the maximum value at pH 8.0 and 6.5 for neutral red and azure-B, respectively, rate decreased with further increase in pH. The results are graphically represented in Fig. 7(a).

The rate of reaction increased on increasing the pH of the medium as the number of ^-OH ions increased with increase in pH, which remained adsorbed on the catalyst making its surface negatively charged. Consequently, a large number of cationic dye molecules approach the catalyst and undergo degradation. But on increasing the pH above optimum values (8.0 and 6.5) dye does not remain in its cationic form at much higher pH. Due to the surrounding envelope of ^-OH ions around dye molecules, their approach towards negatively charged catalyst becomes restricted, and as a result, the rate of degradation of dye starts decreasing on increasing the pH of medium beyond pH 8.0 and 6.0.

Effect of dye concentrations on the rate of photo-Fenton degradation was observed in the range from 0.4×10^{-5} M to 9.0×10^{-5} M (Fig. 7(b)). The rate of degradation increased with an increase in the concentration of neutral red and azure-B up to 7.0×10^{-5} M and 1.2×10^{-5} M, respectively. Further increase in concentration decreased the rate of degradation. This may be explained due to the fact that on increasing the concentration of dye, the rate increases as more molecules of dyes are available for degradation. However, further in-

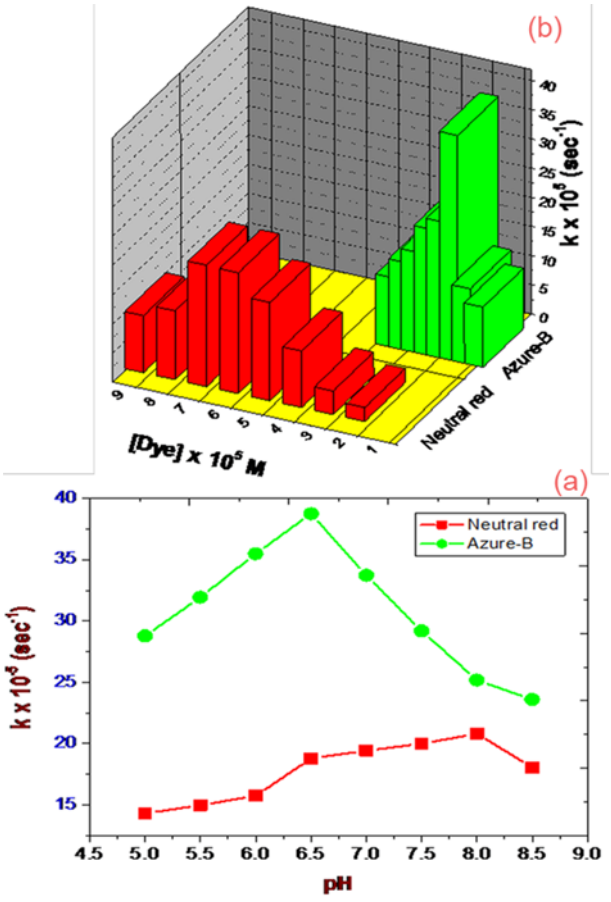

Fig. 7. (a) Effect of pH (Plotted between pH and k×10^5 (sec^{-1}) at optimum conditions for [Neutral red]=7×10^{-5} M, Catalyst =0.05 g, H_2O_2=0.40 mL, Light intensity=70.0 mWcm^{-2} and [Azure-B]=1.2×10^{-5} M, Catalyst=0.06 g, H_2O_2=0.50 mL, Light intensity=60.0 mWcm^{-2}), (b) Effect of dyes concentration (Plotted between [Dye]×10^5 M and k×10^5 (sec^{-1}) at optimum conditions for Neutral red- pH=8.0, Catalyst=0.05 g, H_2O_2=0.40 mL, Light intensity=70.0 mWcm^{-2} and Azure-B- pH=6, Catalyst=0.06 g, H_2O_2=0.50 mL, Light intensity =60.0 mWcm^{-2}).

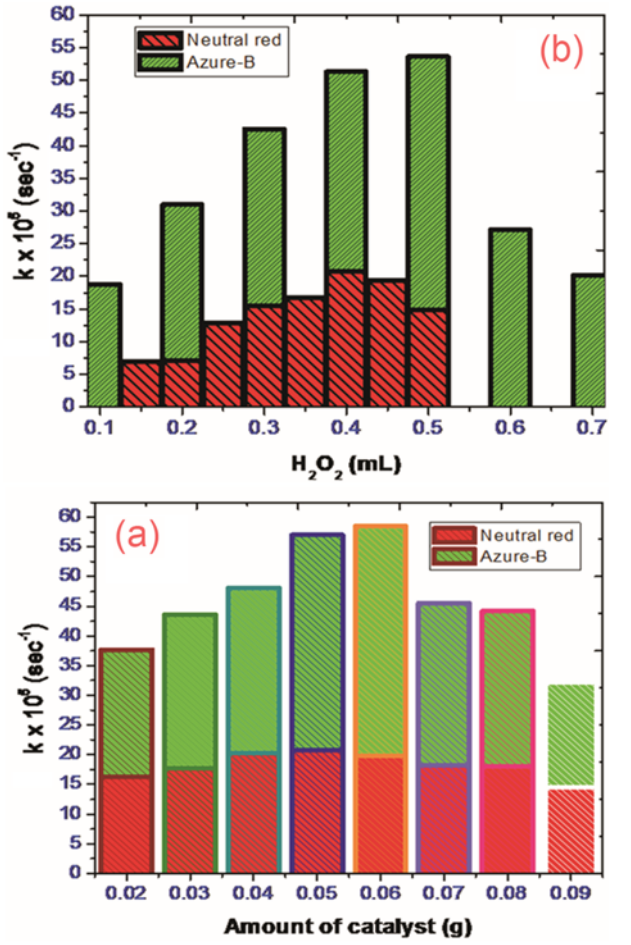

Fig. 8. (a) Effect of amount of catalyst (Plotted between Amount of catalyst (g) and k×10^5 (sec^{-1}) at optimum conditions for [Neutral red]=7×10^{-5} M, pH=8.0, H_2O_2=0.40 mL, Light intensity=70.0 mWcm^{-2} and [Azure-B]=1.2×10^{-5} M, pH=6, H_2O_2=0.50 mL, Light intensity=60.0 mWcm^{-2}), (b) Effect of amount of H_2O_2 (Plotted between H_2O_2 (mL) and k×10^5 (sec^{-1}) at optimum conditions for [Neutral red]=7×10^{-5} M, pH=8.0, Catalyst=0.05 g, Light intensity=70.0 mWcm^{-2} and [Azure-B]=1.2×10^{-5} M, pH=6, Catalyst=0.06 g, Light intensity=60.0 mWcm^{-2}).

crease in concentration beyond optimum concentration causes retardation of reaction due to increase in the number of collisions among dye molecules, whereas collisions among dye molecule and ·OH radicals decrease. As a consequence, rate of reaction is decreased.

The effect of amount of catalyst on the rate of photo-Fenton degradation of dyes was observed by keeping all other factors identical. It is clear from the data that the rate of degradation increases on increasing amount of catalyst up to 0.05 g and 0.06 g for neutral red and azure-B, respectively, which may be regarded as the saturation point. Beyond these values, the rate of reaction decreases with increase in amount of catalyst. This may be explained by the fact that on increase in amount of catalyst there is an increase in surface area of catalyst, leading to increase in rate of reaction. But after a certain limiting amount of catalyst (0.05 g and 0.06 g), if the amount of catalyst is further increased, it would also increase the number of vanadium and copper ions and then there is a possibility of short circuiting of vanadium(IV) & vanadium(V) and cuprous(I) & cupric (II) ions [47,48]. As a result, fewer hydroxyl radicals are formed and reaction rate is retarded (Fig. 8(a)).

The effect of variation of amount of H_2O_2 on the dye degradation was investigated in the range from 0.10 mL to 0.70 mL (Fig. 8(b)). On increasing the amount of H_2O_2, the ·OH radical concentration increased and hence, rate of degradation of dye also increased. At high H_2O_2 concentration, beyond 0.40 and 0.50 mL for neutral red and azure-B, respectively, scavenging of hydroxyl radical also takes place by increasing amount of H_2O_2 generating perhydroxyl radical (Eq. (4)). Perhydroxyl radical is a less strong oxidant as compared to hydroxyl radical. Therefore, the rate of degradation of dye decreases when amount of H_2O_2 is increased beyond 0.40 and 0.50 mL.

$$H_2O_2 + HO^{\bullet} \rightarrow H_2O + HO_2^{\bullet} \quad (4)$$

To observe the effect of intensity of light on the photo-Fenton degradation of dyes, the distance between the light source and the exposed

surface area was varied. With an increase in light intensity, the rate of reaction increased and maximum rates were found at 70.0 and 60.0 $mWcm^{-2}$ for neutral red and azure-B, respectively. The rate of photo-Fenton degradation was accelerated as the intensity of light was increased, because increase in the light intensity will increase the number of photons striking per unit area of catalyst. Further increase in the intensity of light rate of reaction decreases because of thermal side reactions.

3. Quality Parameters of Water

Quality of reaction mixture before and after photo-Fenton degradation was tested by measuring the following parameters:

3-1. Chemical Oxygen Demand (COD)

Chemical oxygen demand of dye solution before and after illumination was determined by redox method. The photodegradation efficiency after 2 hours of illumination was found to be 75% and 60% for neutral red and azure-B, respectively.

3-2. Dissolved Oxygen (DO)

Dissolved oxygen analysis measures the amount of gaseous oxygen dissolved in an aqueous solution. Increase in dissolved oxygen after photo-Fenton degradation indicates mineralization of dye to a significant extent. For neutral red, the DO was 8.0 and 14.6 ppm, respectively, before and after photo-Fenton treatment. On the other hand, DO was 6.2 and 13.6 ppm for azure-B dye.

3-3. Conductivity

Conductivity as a summation parameter is a measure of the level of ions concentration of a solution. Conductivity values increased after the treatment because dye was mineralized into ions like CO_3^{2-}, NO_3^-, SO_3^{2-} etc. The conductivity of neutral red reaction mixture was 126 and 305 μS, respectively, before and after treatment, whereas for azure-B the reaction mixture corresponding values were 117 and 338 μS, respectively. For the same reason, total dissolved solids (TDS) and salinity of the dye solution were found to increase after photo-Fenton degradation of dye.

Before the treatment, pH of reaction mixture is in either acid or basic range (neutral red pH 8.0 and azure-B pH 6.5), but after the degradation of the sample, pH reaches to almost neutral range, because dye particles are mineralized to a significant extent (neutral red pH 7.52 and azure-B pH 7.21).

4. Reusability

The reusability of catalyst is defined as repeated use of recovered catalyst for consecutive runs under the similar experimental conditions ($Cu_3V_2(OH)_2O_7 \cdot 2H_2O$) was immobilized on a glass plate by dip-coating for the repeated use of ($Cu_3V_2(OH)_2O_7 \cdot 2H_2O$) in photo-Fenton processes [49]. The catalytic activity was found to be lower than that of the suspension, because of the decrease of surface area of catalyst in immobilized form. Therefore, centrifugation method was used for the separation of catalyst and its use for further degradation. It has been observed that this method does not affect the efficiency of catalyst very much. After reaction for 30 min, the activity of ($Cu_3V_2(OH)_2O_7 \cdot 2H_2O$) seems to decrease slightly, to around 5% in the 5th run.

5. Mechanism

On the basis of the experimental observations and corroborating the existing literature, a tentative mechanism has been proposed for the degradation of neutral red and azure-B dyes in presence of copper pyrovanadate, H_2O_2 and light. V and Cu may simultaneously activate H_2O_2 to give OH radicals.

$$Cu^{2+} + H_2O \xrightarrow{Visible\ light} Cu^{+} + HO^{\bullet} + H^{+} \quad (5)$$

$$Cu^{+} + H_2O_2 \longrightarrow Cu^{2+} + OH^{-} + HO^{\bullet} \quad (6)$$

$$V^{5+} + H_2O \xrightarrow{Visible\ light} V^{4+} + HO^{\bullet} + H^{+} \quad (7)$$

$$V^{4+} + H_2O_2 \longrightarrow V^{5+} + OH^{-} + HO^{\bullet} \quad (8)$$

This $HO^{\bullet}$ radical is non selective and strong oxidizing agent with relatively high oxidizing potential, as compared to common oxidizing agents like H_2O_2, O_2, O_3 etc. These $HO^{\bullet}$ radicals react with dye molecules and degrade them into smaller products.

$$^1[Dye] \xrightarrow{h\nu} {}^1[Dye]^* \quad (9)$$

$$^1[Dye]^* \xrightarrow{ISC} {}^3[Dye]^* \quad (10)$$

$$^3[Dye]^* + HO^{\bullet} \rightarrow \text{Smaller products} \quad (11)$$

The participation of $HO^{\bullet}$ radicals as an active oxidizing species was confirmed by using hydroxyl radical scavengers, e.g., 2-propanol and butylated hydroxy toluene (BHT), where the rate of photodegradation was found to be drastically reduced.

CONCLUSION

Photo-Fenton reactions are the most effective methods for the treatment of wastewater. In the dark, the rate of Fenton reaction is slow, whereas with the irradiation of reaction mixture with visible light, acceleration in the rate of degradation of dyes was observed. To further increase the activity of photo-Fenton catalyst in heterogeneous phase, many researches are underway by different groups of scientists. Sludge formation of ferrous/ferric hydroxide is a problem at the end of conventional processes of waste water treatment. Utilizing heterogeneous photo-Fenton like reagent can solve this problem to some extent. Thus, in the present work, copper pyrovanadate ($Cu_3V_2(OH)_2O_7 \cdot 2H_2O$) has been used as heterogeneous photo-Fenton like reagent to degrade neutral red and azure-B dyes successfully. The participation of $HO^{\bullet}$ radical as an active oxidizing species was confirmed by carrying out the reaction in the presence of hydroxyl radical scavengers, e.g., 2-propanol and BHT, where the rate of reaction was drastically retarded. Results indicated that simultaneous utilization of all the parameters under optimal conditions increases the degradation of dyes. The dyes quickly lose their color, indicating that the dissolved dyes have been oxidized.

ACKNOWLEDGEMENTS

One of the authors, Sangeeta Kalal, is thankful to University Grants Commission, New Delhi for the award of JRF. We are also thankful to UGC-DAE Consortium, Indore for providing FT-IR and XRD data. Thanks are also due to Head, Department of Chemistry, M.L. Sukhadia University, Udaipur for providing laboratory facilities.

REFERENCES

1. C. Sahunin, J. Kaewboran and M. Hunsom, *Science Asia*, **32**, 181 (2006).
2. U. Pagga and D. Brown, *Chemosphere*, **15**, 479 (1986).
3. J. Feng, X. Hu and P. L. Yue, *Water Res.*, **40**, 641 (2006).
4. R. Ameta, A. Kumar, P. B. Punjabi and S. C. Ameta, in *Adavanced*

Oxidation Processes: Basics and Applications, D. G. Rao, J. A. Byrne, S. Feroz and R. Senthikumar (Eds.), CRC Press, Taylor and Francis, London (2013).
5. H. Zhang, H. J. Choi, P. Canazo and C. P. Huang, *J. Hazard. Mater.*, **161**, 1306 (2009).
6. N. Zhu, L. Gu, H. Yuan, Z. Lou, L. Wang and X. Zhang, *Water Res.*, **46**, 3859 (2012).
7. X. R. Xu, H. B. Li, W. H. Wang and J. D. Gu, *Chemosphere*, **57**, 595 (2004).
8. J. Pignatello, E. Oliveros and A. MacKay, *Crit. Rev. Environ. Sci. Technol.*, **36**, 1 (2006).
9. S.-H. Hong, B.-H. Kwon, J.-K. Lee and I.-K. Kim, *Korean J. Chem. Eng.*, **25**, 46 (2008).
10. P. Vaishnave, A. Kumar, R. Ameta, P. B. Punjabi and S. C. Ameta, *Arab. J. Chem.* In Press (2012).
11. J. X. Chen and L. Z. Zhu, *Chemosphere*, **65**, 1249 (2006).
12. C. B. Molina, J. A. Casas, J. A. Zazo and J. J. Rodriguez, *Chem. Eng. J.*, **118**, 29 (2006).
13. K. M. Parida and A. C. Pradhan, *Ind. Eng. Chem. Res.*, **49**, 8310 (2010).
14. S. Parra, V. Nadtotechenko, P. Albers and J. Kiwi, *J. Phys. Chem. B*, **108**, 4439 (2004).
15. K. Chanderia, S. Kumar, J. Sharma, R. Ameta and P. B. Punjabi, *Arab. J. Chem.*, In Press (2012).
16. B. N. Kumar, Y. Anjaneyulu and V. Himabindu, *J. Chem. Pharm. Res.*, **3**, 718 (2011).
17. J. Sharma, R. Ameta, V. K. Sharma and P. B. Punjabi, *Bull. Catal. Soc. India*, **9**, 99 (2010).
18. N. Ameta, J. Sharma, S. Sharma, S. Kumar and P. B. Punjabi, *Ind. J. Chem.*, **51A**, 943 (2012).
19. B. Iurascu, I. Siminiceanu, D. Vione, M. A. Vicente and A. Gil, *Water Res.*, **43**, 1313 (2009).
20. A. Mamedov and V. C. Corberan, *Appl. Catal. A Gen.*, **127**, 1 (1995).
21. F. Magalhaes, M. C. Pereira, S. E. C. Botrel, J. D. Fabris, W. A. Macedo, R. Mendonc, R. M. Lago and L. C. A. Oliveira, *Appl. Catal. A Gen.*, **332**, 115 (2007).
22. Y. Zhang, X. M. Dou, J. Liu, M. Yang, L. P. Zhang and Y. C. Kamagata, *Catal. Today*, **126**, 387 (2007).
23. R. C. C. Costa, M. F. F. Lelis, J. D. Fabris, J. D. Ardisson and L. C. A. Oliveira, *J. Hazard. Mater.*, **129**, 171 (2006).
24. V. S. Teresa, V. V. Patricia, A. L. Sonia and M. A. F. Gregorio, *Catal. Commun.*, **8**, 2037 (2007).
25. P. Baldrian, V. Merhautova, J. Gabriel, F. Nerud, P. Stopka, M. Hruby and J. B. Milan, *Appl. Catal. B Environ.*, **66**, 258 (2006).
26. R. Gopinath, A. R. Paital and B. K. Patel, *Tetrahedron Lett.*, **43**, 5123 (2002).
27. S. Shylesh and A. P. Singh, *J. Catal.*, **228**, 333 (2004).
28. L. Rout and T. Punniyamurthy, *Adv. Synth. Catal.*, **347**, 1958 (2005).
29. C. X. Yin and R. G. Finke, *J. Am. Chem. Soc.*, **127**, 13988 (2005).
30. J. Kasai, Y. Nakagawa, S. Uchida, K. Yamaguchi and N. Mizuno, *Chem. Eur. J.*, **12**, 4176 (2006).
31. R. Z. Khaliullin, A. T. Bell and M. Head-Gordon, *J. Phys. Chem. B.*, **109**, 17984 (2005).
32. P. Y. Zavalij, F. Zhano and M. S. Whitingham, *Acta Cryst.*, **C53**, 1738 (1997).
33. M. Machida, Y. Miyazaki, Y. Matsunaga and K. Ikeue, *Chem. Commun.*, **47**, 9591 (2011).
34. P. Kaur, A. Khant and R. C. Khandelwal, *Int. J. Chem. Sci.*, **9**, 980 (2011).
35. D. Sharma, A. Bansal, R. Ameta and H. S. Sharma, *Int. J. Chem. Technol. Res.*, **3**, 1008 (2011).
36. B. Pare, V. Singh and S. B. Jonnalagadda, *Ind. J. Chem.*, **50A**, 1061 (2011).
37. E. Rosales, M. Pazos, M. A. Sanromán and T. Tavares, *Desalination*, **284**, 150 (2012).
38. Y. Jhala, A. K. Chittora, K. L. Ameta and P. B. Punjabi, *Int. J. Chem. Sci.*, **8**, 1389 (2010).
39. B. Pare, P. Singh and S. B. Jonnalagadda, *Ind. J. Chem. Technol.*, **17**, 391 (2010).
40. N. Ameta, S. Kalal, R. Ameta, A. K. Chittora and P. B. Punjabi, *Int. J. Chem.*, **1**, 337 (2012).
41. T. Zhang, C. Li, J. Ma, H. Tian and Z. Qiang, *Appl. Catal. B: Environ.*, **82**, 131 (2008).
42. S. Xing, C. Hu, J. Qu, H. He and M. Yang, *Environ. Sci. Technol.*, **42**, 3363 (2008).
43. Y. E. Zeng, H. S. Zhang and Z. H. Chen, Handbook of Organic Reagents, Chemical Industry Press, Beijing, **4**, 793 (1989).
44. E. Tuite and J. M. Kelly, *Biopolymers*, **35**, 419 (1995).
45. B. K. Hordern, M. Ziołek and J. Nawrocki, *Appl. Catal. B: Environ.*, **46**, 639 (2003).
46. M. A. Lafontaine, A. Le Bail and G. Ferey, *J. Solid State Chem.*, **85**, 220 (1990).
47. D. Klauson, S. Preis, E. Portjanskaja, A. Kachina, M. Krichevskaya and J. Kallas, *Environ. Technol.*, **26**, 653 (2005).
48. M. J. L. Munoz, J. Aguado and B. Ruperez, *Res. Chem. Intermed.*, **33**, 377 (2007).
49. C. He, Y. Xiong and X. Zhu, *Appl. Catal. A Gen.*, **275**, 55 (2004).